NASA Technical Memorandum 82757

Geometrical Aspects of the Tribological Properties of Graphite Fiber Reinforced Polyimide Composites

Robert L. Fusaro
Lewis Research Center
Cleveland, Ohio

Prepared for the
1982 Annual Meeting of the American Society
of Lubrication Engineers
Cincinnati, Ohio, May 10–13, 1982

NASA

GEOMETRICAL ASPECTS OF THE TRIBOLOGICAL PROPERTIES OF GRAPHITE FIBER REINFORCED POLYIMIDE COMPOSITES

by Robert L. Fusaro

National Aeronautics and Space Administration

Lewis Research Center

Cleveland, Ohio

ABSTRACT

A Latin Square statistical experimental test design was used to evaluate the effect of temperature, load and sliding speed on the tribological properties of graphite fiber reinforced polyimide (GFRPI) composite specimens. Hemispherically tipped composite riders were slid against 440C HT stainless steel disks. Comparisons were made to previous studies in which hemispherically tipped 400C HT stainless steel riders were slid against GFRPI composite disks and to studies in which GFRPI was used as a liner in plain spherical bearings. The results indicate that sliding surface geometry is especially important, in that different geometries can give completely different friction and wear results. Load, temperature, and sliding distance were found to influence the friction and wear results but sliding speed was found to have little effect. Experiments on GFRPI riders with 10 weight percent additions of graphite fluoride showed that this addition had no effect on friction and wear.

INTRODUCTION

The use of polymer-matrix composite materials for self-lubricating applications is continually increasing, particularly in the aerospace industry. Because of this, considerable research has been conducted on reinforced polymers (Refs. 1-16). Fiber reinforced polymers are especially

useful because fibers improve the strength and stiffness of the composite and offer improved load carrying capacity. In addition, graphite fibers offer improved lubricating performance, due to their good tribological properties.

Many of the applications for these composite materials are at elevated temperatures, thus, it is desirable to use the most thermally stable polymers available which also have good tribological properties. One of the most thermally stable polymers with good lubricating properties is the class of polymers known as polyimides. Previous studies (11-15, 18) on graphite fiber reinforced polyimide (GFRPI) composites have shown this material has considerable promise for self-lubricating applications up to 340° C.

In addition to elevated temperatures, these composite materials will be used under a variety of sliding conditions, such as different geometries, temperatures, speeds, and loads. Thus, the purpose of this study was to do a fundamental investigation of how these parameters can affect friction, wear, surface morphology and transfer.

To accomplish this, a Latin-square statistical experimental design was used. This was done to reduce the total possible experimental combination of variables (64) down to a more reasonable number (16). A pin-on-disk type of friction and wear apparatus was used to conduct the experiments. The pin was made from GFRPI and the disk was made of AISI 440C HT (high temperature) stainless steel.

In addition to the above parameters, the effect of sliding duration was also investigated by sliding selected experimental conditions much greater distances. The effect of geometry was investigated by comparing the results

of this study to previous work in which a metal rider slid against a GFRPI disk (15), and to plain spherical bearing experiments (13).

In addition to the proceeding experiments, similar experiments were also conducted on a modification of the GFRPI composite material by adding 10 percent (by weight) of graphite fluoride $[(CF_{1.1})_n]$ powder to it.

MATERIALS

The composite material evaluated in this study was made from a 50/50 (by weight) mixture of graphite fibers and polyimide resin. The graphite fibers were 6.4×10^{-3} m long and 7.6×10^{-6} m in diameter. The fiber was designated as type "L" in Ref. 15 and had a relatively low tensile strength and elastic modulus. Table 1 lists typical properties of the fiber. The polyimide resin used was an addition-type (designated type "A" in Ref. 15) whose molecular structure was highly crosslengthed. The structure is given in Fig. 1. An advantage of addition-type polyimides is that they do not release water vapor during polymerization. Water release can cause voids in the final cured polymer. Polymerization chemistry and cure procedures are given in Refs. 14 and 17.

The fibers were randomly dispersed thoughout the polyimide matrix and transfer molded into hemisphereically tipped (0.476 cm-diameter) riders. See Ref. 18 for molding procedure. Actually, the fibers were not completely randomly dispersed, since some preferred ordering likely occurred during molding and the fibers tended to cluster together. A modification of the above composite material was made by adding 10 percent (by weight) of well-dispersed graphite fluoride $(CF_{1.1})_x$ powder to it.

The disk material was AISI 440C HT (high temperature) stainless steel, which was hardened to Rockwell C-60. They were lapped and polished to a

centerline average (CLA) surface finish of 10^{-7} meter (4 μin.). Cleaning with levigated alumina did not change this value.

APPARATUS

A pin-on-disk type of friction and wear apparatus was used in this study. The friction specimens (Fig. 2) consisted of a stationary (0.476 cm radius) hemispherically tipped GFRPI rider in sliding contact with a flat (6.3 cm diam) 440C HT stainless steel disk. The apparatus was equipped with a variable-speed motor and gear reduction system so that rotational speed could be controlled. The rider slid on a 5.2 cm diameter circular track on the disk. The disk was heated by a high frequency induction unit. The temperature of the disk was monitored by a thermocouple when the disk was not rotating and by an infrared pyrometer when it was in motion. The friction specimens were enclosed in a chamber in order to control the atmosphere at 10 000 ppm H_2O (50 percent R.H at 25° C).

PROCEDURE

Specimen Cleaning

The AISI 440C HT stainless steel disks were cleaned by washing with ethyl alcohol and then by scrubbing with a water paste of levigated alumina. They were then scrubbed with a brush under running distilled water to remove the levigated alumina, and dried with clean compressed air.

The GFRPI riders were scrubbed with a nonabrasive detergent, rinsed with distilled water and dried with clean compressed air.

Experimental Testing

In order to determine the effect of sliding speed, load and temperature on the friction coefficient and GFRPI rider wear rate, a Latin-square factorial experimental plan (19) was used. It is possible to use this type of

experimental plan since it can be assumed that the dependent result R (friction coefficient or GFRPI wear rate) is a function of the product of the individual functions of the independent variables X (load), Y (sliding speed), and Z (temperature), or

$$R = f_1(X)f_2(Y)f_3(Z) \qquad (I)$$

where f_1, f_2, and f_3 are functions of any level of complexity. This equation can be transformed to the form

$$\log R = \log f_1(X) + \log f_2(Y) + \log f_3(Z) \qquad (II)$$

It can be proved (19), that if the logarithms of the results are numerically averaged over a single value of X, Y, or Z, that the effects of those factors that are changing (such as Y and Z for the X matrix level) will remain the same form one level (X level) to the next. In order words, all changes in the logarithmic average (geometric mean) of the X level results are wholly due to the effect of X alone. The same is true for the Y and Z levels. Thus it is possible to obtain tabulations or curves of R as a function of X, Y, and Z separately such as

$$R_x = k\, f_1(X)$$

$$R_y = k' f_2(Y) \qquad (III)$$

$$R_z = k'' f_3(Z)$$

where k, k', and k" are constants and R_x is the antilog of $\sum \log R_x/n$, etc., where n equals the number of matrix levels.

The preceeding three equations can be solved for $f_1(X)$, $f_2(Y)$, and $f_3(Z)$ to yield

$$R = K(R_x)(R_y)(R_z) \qquad (IV)$$

where K is $(kk'k")^{-1}$. K can be evaluated if the final result R is known and the individual R's from the X,Y,Z curves are known. An example of this method for the GFRPI rider wear rates will be shown in a following section.

The Latin-square test matrix and the variables used for sliding speed, load and temperature are give in Table 2. The sliding duration for the Latin-square experiments was 1 kilometer. The tests were stopped after 3, 15, 50, 100, 200, 400, and 1000 meters for the 0.014 and the 0.14 m/s sliding speed experiments. For the 1.7 and 2.7 m/s sliding speed experiments the tests were stopped after 40, 200, 400, 600, 800, and 1000 meters. It was determined that "run-in" took place in less than 3 meters of sliding. From that point, the wear rate for each experimental condition was relatively constant. The values presented for the GFRPI rider wear rates for each test are a least squares fit of the data.

During the intervals when the tests were stopped, the contact areas were examined by optical microscopy and the wear volume was determined by measuring the wear scar on the hemispherically tipped rider and calculating the volume of material worn away. The rider was not removed from the holder and locating pins insured that it was returned to its original position when it was put back into the apparatus. To determine the effect of sliding distance, four experimental conditions from the Latin-square matrix were selected for longer duration testing (up to 19 km). The same experimental method was followed.

RESULTS AND DISCUSSION

LATIN SQUARE EVALUATION

Friction Coefficient

Friction coefficients (the average and the variation) for each Latin-square experimental condition (Table 2) are given in Table 3. Table 3A lists the results for the case when no solid lubricants were added to the composites and Table 3B lists the results when a 10-percent weight addition of graphite fluoride was added to the composites.

If the general Eq. (I) governs this experiment, a logarithmic average (geometric mean) can be taken. Figures 3 to 5 give the geometric mean of the friction coefficient data as a function of sliding speed, load, and temperature respectively. The curves can not be used directly to give, for example, a value for the friction coefficient at a constant load, since they represent averages rather than discrete values. But, since the log-averaging process eliminates the effect of the other two variables, generalizations on the effect of each variable can be made. It is possible to obtain useful numerical values for the friction coefficient from the curves (for experimental conditions not evaluated) by using Eq. (IV); but since friction coefficient was so highly dependent on sliding distance, this was not attempted. The technique was used for wear rate calculations, however.

Figures 3 to 5 indicate that graphite fluoride additions had no effect on the friction coefficient. The figures also indicate, that sliding speed in the range of 0.014 to 2.8 m/s and load in the range of 2.0 to 19.6 N had little effect on friction coefficient. Temperature (Fig. 5), however, had a very marked effect on the friction coefficient. The average friction coefficient increased with increasing temperature as did the variation of

friction coefficient at constant temperature. The variation in Fig. 5 was most affected by sliding distance, especially at elevated temperatures. Figure 6 gives typical friction traces at a sliding speed of 1.7 m/s, showing the effect of sliding distance and temperature on friction coefficient.

Wear

No detectable wear occurred on the 440C HT stainless steel disks. The wear rates for GFRPI riders without and with graphite fluoride additives are given for each Latin-square experimental condition in Tables 3A and 3B respectively. Geometric means of the rider wear rates were calculated and are plotted as a function of sliding speed, load, and temperature, respectively, in Figs. 7 to 9.

As found for the friction coefficients, 10 weight percent additions of graphite fluoride did not noticeably affect rider wear rates. Also sliding speed had little effect on wear rate between 0.14 to 2.8 m/s (Fig. 7). At the slowest experimental speed (0.014 m/s), however, the wear rate was found to be approximately double that at the higher speeds. Figure 8 indicates wear rate increased in a linear manner with increasing load, and Fig. 9 indicates wear rate increased in an exponential manner with increasing temperature.

As mentioned previously, useful interpretation of these curves can be obtained from Eq. (IV) if the unknown constant K is calculated. The value of K can be calculated for each set of experimental conditions in the Latin-square. The differences in the various K's calculated give an indication of how the data deviates from the ideal of Eq. (I). Table 4A shows the K values calculated for the 16 experiments conducted with no graphite fluoride additions and Table 4B shows similar K values calculated for

10 weight percent additions of graphite fluoride. The average value of K for the experiments with no graphite fluoride additions was 1.6×10^{27} and the maximum deviation was 0.9×10^{27} or 56 percent. The average value of K for the experiments with 10 weight percent additions of graphite fluoride was 1.5×10^{27} and the maximum deviation was 1.1×10^{27} or 73 percent.

While this is quite a large uncertainty figure, it is not surprising, since wear is dependent on many variables which may not have been taken into account. Some possible reasons for the deviation may have been due to the fact that the experimental plan included a temperature (350° C) which was above the T_G of the polyimide, fiber orientation in the composites may have been different for the different individual tests, there may have been slight undetectable differences in surface topography, graphite fluoride powder may have not been evenly dispersed, etc.

The advantage of the method is that the average value of K can be used to calculate wear rates for experimental conditions (within the matrix) not evaluated. This is done by substituting wear rate values from the individual curves into Eq. (IV).

LONGER DURATION EVALUATION

A selected number of experiments were continued past the cutoff sliding distance of 1 km used in the Latin-square evaluations. This was done to determine the effect of sliding distance and decreasing contact stress (or increasing rider contact area) on GFRPI rider wear rates and friction coefficients. Table 5 presents the results of these experiments. Only the GFRPI riders without solid lubricant additives were evaluated in these experiments. The temperature and load conditions evaluated were (25° C,

19.6 N); (100° C, 9.8 N); (200° C, 4.9 N); and (350° C, 2.0 N). A constant speed of 1.7 m/s was employed.

For each experimental condition mentioned above, the friction coefficient increased for sliding distances greater than 1 km. The friction coefficient eventually came to an equilibrium value, but the distance at which this occurred depended on the experimental conditions.

Apparent contact stress values were calculated at the end of each sliding interval from the GFRPI rider wear scar areas, and the values are given in Table 5. In general, the friction coefficients and the GFRPI wear rates increased with sliding duration, which indicates either decreasing apparent contact stress or the corollary, increasing apparent contact area, were responsible for the higher friction and wear. A possible explanation for this in terms of surface morphology will be discussed in a following section.

GFRPI SURFACE MORPHOLOGY

The morphology of the wear surfaces on the GFRPI riders was found to be influenced primarily by temperature. The other experimental conditions, including sliding distance, had a minimal effect on the surface morphology of GFRPI riders.

Figure 10 gives representative photomicrographs of the GFRPI rider contact areas which are typical of all the experiments at 25° C. A very smooth wear surface is seen. The graphite fibers are very distinct from the polyimide matrix and no sintering of constituents was observed. The lighter colored particles observed in the polyimide matrix are imbedded polyimide or graphite fiber wear particles.

Fiber wear appeared to be independent of fiber orientation, that is whether they were parallel, perpendicular, or oblique to the surface did not

appear to affect the wear properties of the fibers. The fibers were worn very smooth and there were no observable differences in the surface morphological appearance that depended upon orientation. Figure 10 indicates that true random orientation of the fibers did not occur. The fibers tended to cluster together in bunches which had different orientations.

Figure 11 gives representative photomicrographs of the GFRPI riders for experiments at 100° C. At 100° C, the graphite fibers tended to breakup, and spall from the surface; especially so, when they were parallel to the sliding interface (Fig. 11). Except for this, the surfaces looked very similar to those at 25° C. An observation was that increasing the load tended to increase the rate at which the fibers broke up.

Similar surfaces to those at 100° C were observed at 200° C, but with the observation that the fibers tended to break up at a faster rate. At 350° C, a different phenomenon occurred and that was the polyimide polymer itself tended to breakup or degrade. This is not surprising, since 350° C is above the T_G of this polyimide. Figure 12 gives representative photographs of the GFRPI rider surfaces at 350° C. Figure 12(b) indicates that the polyimide is tending to break away from the fibers which are perpendicular or oblique to the surface. Figure 12(a) displays areas where large clusters of fibers parallel to the surface have broken away from the surface. The surfaces of the fibers themselves have the same appearance as they had at the lower temperatures, but the polyimide surface has lost its smooth character and is rough and cracked.

Morphologically, the polyimide wear surface looked very similar at 25° C, 100° C, and 200° C; nevertheless undetected changes in the polyimides structural properties due to additional frictional heating at these tempera-

tures may have been the cause of the graphite fibers parallel to the sliding interface breaking up and spalling. The study indicates that fibers parallel to the sliding interface are not desirable from a wear point of view since they have a tendency to spall.

TRANSFER FILMS

Transfer appeared to increase with both temperature and sliding distance. No correlation with load or speed was observed under the conditions of these experiments. Since projected contact stress decreased and apparent area of contact increased with sliding duration, it is possible that these two parameters may also have influenced transfer.

Representative photomicrographs of the transfer to the 440C HT stainless steel disks at 25° C after 1 km of sliding is shown in Fig. 13(a). The transfer is plate-like and interference fringes can be seen in the platelets, indicating the thickness is 0.8 micrometers (wavelength of red light) or less.

As sliding distance or temperature increased, the transfer tended to build up, giving the surface a rough appearance. The transfer looked like a mountainous region with flat plateaus on the peaks. Figure 13(b), gives a representative photomicrograph of this type of transfer, it was taken after 1 kc of sliding at 350° C under a 1 kg load and 1.7 m/s sliding speed.

Correlation of this transfer build up phenomenon to the friction and wear properties indicates that the buildup of thick transfer films is detrimental to friction and wear properties of GFRPI composites. It is believed that transfer films are necessary for good lubrication; but, they must be in the form of thin plastically flowing films. If they are too thick, instead

of shearing at the interface, they adhesively "pluck" material from the composite, thereby increasing friction and wear.

GEOMETRY EFFECTS

In Ref. 15, the same GFRPI composite material used in this study was molded into a disk and a 440C HT stainless steel rider was slid against it. In Ref. 13, the same GFRPI composite material was evaluated both as a molded liner and as an insert liner in a self-aligning plain bearing. The friction and wear results of this study were compared to those of the two previous studies and the results are given in Table 6.

It is interesting to note that the friction and wear results from the self-aligning plain bearing experiments and from the pin-on-disk experiments compare very closely when a hemispherically tipped metal pin slid against the composite disk. But, when a hemispherically tipped GFRPI rider was slid against a metal disk, the friction and wear results were entirely different. It is believed that the reasons for these differences were due to differences in surface morphology (caused by geometry effects), in transfer films, in projected contact stresses, and possibly to temperature differences in the contact area.

Representative photomicrographs of the GFRPI disk wear track surfaces are shown in Fig. 14 at (a) 25° C and at (b) 300° C after 50 km of sliding. At 25° C (Fig. 14(a)), the graphite fibers are distinguishable, but there is no sharp distinction between the fibers and the polyimide matrix as was found when the GFRPI riders slid on the metallic disk (Fig. 10). On the composite disk, the wear particles from the graphite fibers and from the polyimide have mixed together to form a thin, plastically flowing film.

At 300° C, the GFRPI disk produced surfaces somewhat similar to those of the rider, but the tendency for the fibers to spall from the polyimide matrix was not as great. Generally only fibers parallel to the sliding surface spalled. Figure 14(b) shows a typical fiber spall. It is not clearly seen in Fig. 14(b), but at 300° C the polyimide material tended to flow over and across the graphite fibers. Since some polyimides have very low friction properties at 150° C and above (20), it is postulated that the low friction obtained with the plain spherical bearing and with the metal pin on GFRPI disk experiments is due to the polyimide dominating the results.

Another difference is in the transfer film properties. As previously mentioned, the transfer from the GFRPI pin to the metallic disk tended to buildup with sliding distance or with temperature (Fig. 13) and as this occurred the friction coefficient increased. But this did not occur with the metal pin sliding on the GFRPI disk. Transfer films tended to be 0.4 to 0.8 μm (wavelength of light) thick and tended to plastically flow across the rider contact area. Also friction coefficient tended to remain constant with increasing sliding distance (up to 50 km of sliding) and to decrease with increasing temperature.

Lancaster (16) has also studied geometrical effects on the wear of polymers. He concluded that abrasive wear is important in the early stages of sliding and that volumetric wear is dependent on load rather than nominal pressure. In general, the author agrees with this, except that during the initial stages of sliding, the author believes that pressure can also be a dominating factor in the wear process, especially with hemispherically tipped composite riders or polymers. If the contact pressure is higher than the yield stress of the composite (under sliding conditions), it will deform

or wear rapidly until some equilibrium pressure is reached. Below this pressure value, wear is a constant function of load. This pressure effect was shown in Ref. 21, where the wear rate of polyimide-bonded graphite fluoride films was shown to increase at a constant rate as a function of load below a certain pressure for a constant projected contact area; but above this pres- sure, wear rate increased exponentially.

Lancaster (16) also states that "the size of the contact area may affect the localized temperature rise at the asperity contacts by influencing the number, size, and distribution of these contacts." This may be a possible reason for the friction and wear rates increasing with sliding distance in these experiments. The author believes that contact pressures may also have been responsible. When contact pressures are high, the transfer film is sheared in the sliding process, but when contact pressures drop due to the wear of the rider, instead of shearing, the transfer film tends to adhesively wear the composite rider.

For the longer duration experiments the projected contact stress at the end of each sliding interval was calculated from the GFRPI circular wear scars (table 5). The stress varied from 34 MPa (5000 psi) to 0.4 MPa (60 psi). The stress was constant for the journal bearing (28 MPa). For the metal rider sliding on the GFRPI disks, the value after run-in varied from 56 MPa to 28 MPa.

Summing up the geometry effects, it is seen that a small metallic contact sliding against a composite tends to act like a plow, creating a furrow and mixing the constituents of the composite together. Since the metallic contact is small and there is a converging inlet, wear particles tend to buildup in the inlet and are compacted and compressed as they plastically

flow into the contact area. As long as contact stresses are high enough, very thin plastic films flow across the contact area. The material on the disk also flows, but only a short distance since the rider contact time is small.

A composite rider sliding on a metal disk first must elastically and or plastically deform to support the load. Instead of a furrow on the disk, a flat is worn on the rider. Also, since the composite contact area is small compared to the metallic area, a longer time is needed to establish a transfer film. Transfer is continually being deposited on the metallic disk surface, and tends to build up with repeated passes. It is believed that when the transfer becomes too thick, it loses its tendency to plastically flow or shear and tends to adhesively pluck material from the composite rider.

CONCLUSIONS

Friction, wear, and optical microscopy studies of hemispherically tipped graphite fiber reinforced polyimide (GFRPI) composite riders sliding against 440C stainless steel disks were conducted and the results compared to previous studies in which hemispherically tipped metallic riders were slid against GFRPI disks and to studies in which the GFRPI was evaluated as a liner in a plain spherical bearing. The results indicate that:

1. It is very important to evaluate polymeric tribological materials with a geometry that is similar to the intended end use, since the friction wear, and wear surface morphological characteristics are highly dependent on the specimen sliding configuration.

2. By evaluating polymeric materials with different sliding configurations, it might be possible to infer design changes in the intended and use which could produce improved performance.

3. GFRPI composite friction and wear results from a pin-on-disk accelerated test apparatus showed good correlation to an end use application (plain spherical bearing) when the disk was made from the composite and a metal rider slid against it. A GFRPI rider sliding against a metal disk, showed poor correlation.

4. GFRPI composite rider wear rates and average friction coefficients tended to increase with sliding distance. This was associated with the build up of thick transfer films which instead of shearing at the interface, adhesively "plucked" material from the composite.

5. Ten weight percent graphite fluoride powder additions to the composites had little or no effect on the friction and wear results.

6. A Latin-square statistical experimental test design gave a good indication of the general effect of sliding speed, load, and temperature on the GFRPI rider friction and wear results, and reduced the total possible combination of variables from 64 to 16.

7. With proper use of the Latin-square method, it is possible to predict friction and wear results for experimental conditions not evaluated.

REFERENCES

1. Giltrow, J. P. and Lancaster, J. K., "Properties of Carbon-Fibre-Reinforced Polymers Relevant to Applications in Tribology," London, Plastics Institute, International Conference on Carbon Fibres, Their Composites and Applications, February 1971, Paper 31.
2. Giltrow, J. P. and Lancaster, J. D., "Friction and Wear of Polymers Reinforced with Carbon Fibers," Nature 214, 1106-1107 (1967).
3. Lancaster, J. K., "The Effect of Carbon Fibre Reinforcement on the Friction and Wear of Polymers," J. Phys. D. 1, 549-559 (1968).

4. Giltrow, J. P., "A Design Philosophy for Carbon Fibre Reinforced Sliding Components," Tribology 4, (1) 21-28 (1971).

5. Harris, C. L. and Wyn-Roberts, D., "Wear of Carbon Fibre Reinforced Polymers in a High Vacuum Environment," Nature 217, 981-982 (1968).

6. Giltrow, J. P. and Lancaster, J. K., "Carbon-Fibre Reinfored Polymers as Self-Lubricating Materials," Tribology Convention, Pithochry, Scotland, May 15-17, 1968, Proceedings, Institution of Mechanical Engineers, pp. 149-159 (1968).

7. Giltrow, J. P. and Lancaster, J. K., "The Role of the Counterface in the Friction and Wear of Carbon Fibre Reinforced Thermosetting Resins," Wear 16, (11) 359-374 (1970).

8. Simon, R. A. and Prosen, S. P., "Graphite Fiber Composites; Shear Strength and Other Properties," Twenty-Third Annual Technical Conference, SPI Reinforced Plastics Composite Division, Proceedings, Society of the Plastics Industry, Inc., Section 16-B, pp. 1-10 (1968).

9. Herrick, J. W., "Bearing Materials from Graphite Fiber Composites," Reinforced Plastics - Ever New; Proceedings of the Twenty-Eighth Annual Technical Conference, Society of the Plastics Industry, Inc., 17-D, 1-17-D, 6 (1973).

10. Giltrow, J. P., "The Influence of Temperature on the Wear of Carbon Fiber Reinforced Resins," ASLE Trans. 16, (2) 83-90 (1973).

11. Sliney, H. E. and Johnson, R. L., "Graphite Fiber-Polyimide Composites for Sperical Bearings to 340 C (650 F)," NASA TN D-7078 (1972).

12. Sliney, H. E., Jacobson, T. P., and Munson, H. E., "Dynamic Load Capacities of Graphite-Fiber - Polyimide Composites in Oscillating Plain Bearings to 340 C (650 F)," NASA TN D-7880 (1975).

13. Sliney, H. E. and Jacobson, T. P., "Performance of Graphite Fiber-Reinforced Polyimide Composites in Self-Aligning Plain Bearings to 315° C," Lubr. Eng. 31, (12) 609-613 (1975).

14. Sliney, H. E. and Jacobson, T. P., "Some Effects of Composition on Friction and Wear of Graphite-Fiber-Reinforced Polyimide Liners in Plain Spherical Bearings," NASA TP 1229 (1978).

15. Fusaro, R. L. and Sliney, H. E., "Friction and Wear Behavior of Graphite Fiber Reinforced Polyimide Composites," ASLE Trans., 21 (4) 337-343 (1978).

16. Lancaster, J. K., "Geometrical Effects on the Wear of Polymers and Carbons," Lubr. Technol., 97 (2) 187-194 (1975).

17. Ciba - Geigy Bulletin "P105A Polyimide Laminated Varnish," Ciba - Geigy Corp., Ardsley, NY, 1972.

18. Sliney, H. E., "Some Load Limits and Self-Lubricating Properties of Plain Spherical Bearings with Molded Graphite Fiber-Reinforced Polyimide Lines to 320° C," Lubr. Eng., 35 (9) 497-502 (1979).

19. Schenck, H. Jr., Theories of Engineering Experimentation, McGraw-Hill, 1961.

20. Fusaro, R. L., "Polyimide Film Wear - Effect of Temperature and Atmosphere," NASA TN D-8231 (1976).

21. Fusaro, R. L., "Effect of Load, Area of Contact, and Contact Stress on the Tribological Properties of Polyimide Bonded Graphite Fluoride Films," Wear of Material 1981, ASME, pp. 625-636 (1981).

TABLE 1. - TYPICAL GRAPHITE FIBER PROPERTIES

Property or characteristic	Type "L"	
	English units	SI units
Tensile strength	9.0×10^4 lb/in^2	6.2×10^8 N/m^2
Elastic modulus	5.0×10^6 lb/in^2	3×10^{10} N/m^2
Length	0.25 in.	6.4×10^{-3} m
Diameter	3.3×10^{-4} in.	8.4×10^{-6} m
Specific gravity	1.4	1.4

TABLE 2. - LATIN-SQUARE TEST MATRIX

Speed, m/s	Temperature, °C			
	25	100	200	350
0.014	C	D	A	B
0.14	B	A	D	C
1.7	D	C	B	A
2.8	A	B	C	D

Symbol	Load, N
A	2.0
B	4.9
C	9.8
D	18.6

TABLE 3. - SUMMARY OF LATIN-SQUARE EXPERIMENTAL DATA AND RESULTS

Part A - No Solid Lubricant Additions

Experimental conditions			Friction coefficient		Rider wear rate, m^3/m
Temperature, °C	Load, N	Speed, m/s	Average	Variation	
25	2.0	2.8	0.30	0.20 - 0.32	1.3×10^{-15}
	4.9	.14	.25	.16 - 0.28	1.0
	9.8	.014	.24	.22 - 0.31	5.4
	19.6	1.7	.17	.15 - 0.20	2.5
100	2.0	0.14	0.30	0.16 - 0.44	4.4×10^{-15}
	4.9	2.8	.32	.12 - 0.35	11
	9.8	1.7	.25	.14 - 0.29	18
	19.6	.014	.33	.17 - 0.38	120
200	2.0	0.014	0.50	0.36 - 0.80	34×10^{-15}
	4.9	1.7	.40	.30 - 0.49	68
	9.8	2.8	.52	.26 - 0.60	57
	19.6	.14	.50	.30 - 0.68	89
350	2.0	1.7	1.00	0.45 - 1.16	140×10^{-15}
	4.9	.014	.80	.28 - 1.70	260
	9.8	.14	.70	.18 - 0.90	230
	19.6	2.8	.42	.27 - 0.57	320

TABLE 3. - CONCLUDED.

Part B - Ten Weight Percent Graphite Fluoride Additions

Experimental conditions			Friction coefficient		Rider wear rate, m^3/m
Temperature, °C	Load, N	Speed, m/s	Average	Variation	
25	2.0	2.8	0.24	0.18 - 0.26	0.5×10^{-15}
	4.9	.14	.25	.18 - 0.30	1.5
	9.8	.014	.20	.17 - 0.26	1.3
	19.6	1.7	.18	.17 - 0.19	9.2
100	2.0	0.14	0.30	0.14 - 0.38	8.8×10^{-15}
	4.9	2.8	.33	.13 - 0.36	12
	9.8	1.7	.34	.13 - 0.38	23
	19.6	.014	.34	.18 - 0.50	65
200	2.0	0.014	0.30	0.26 - 0.46	79×10^{-15}
	4.9	1.7	.50	.36 - 0.66	53
	9.8	2.8	.50	.20 - 0.77	62
	19.6	.14	.50	.12 - 0.82	83
350	2.0	1.7	.95	0.60 - 1.05	72×10^{-15}
	4.9	.014	.50	.27 - 0.60	270
	9.8	.14	.70	.35 - 0.90	220
	19.6	2.8	.72	.50 - 0.75	440

TABLE 4. - VALUES OF K CALCULATED

FROM EQUATION (IV)

Part A - No Solid Lubricant Additives

Speed, m/s	Temperature, °C			
	25	100	200	350
0.014	1.6×10^{27}	2.5×10^{27}	0.9×10^{27}	1.1×10^{27}
0.14	1.3	1.1	1.6	1.7
1.7	0.9	1.2	2.2	1.9
2.8	2.2	1.3	1.3	1.1

Part B - Ten Weight Percent Graphite

Fluoride Additions

Speed, m/s	Temperature, °C			
	25	100	200	350
0.014	1.1×10^{27}	1.6×10^{27}	2.5×10^{27}	1.4×10^{27}
0.14	1.7	0.9	1.2	1.6
1.7	0.8	1.5	1.8	1.9
2.8	2.6	1.3	0.8	1.5

TABLE 5. - FRICTION AND WEAR RESULTS FOR LONGER SLIDING DURATIONS

Experimental conditions		Sliding interval, km	Friction coefficient		Contact stress (end of interval)		Wear rate	
			Average	Variation			m^3/kc	m^3/m
Ambient temperature, °C	Load, N				MPa	psi		
25	19.6	0 - 1	0.17	0.15 - 0.20	34	5000	0.40×10^{-12}	2.5×10^{-15}
		1 - 2	.20	.18 - 0.24	30	4400	.67	4.3
		2 - 3	.19	.17 - 0.26	24	3500	.56	3.6
		3 - 4	.20	.19 - 0.21	18	2600	.82	5.2
		4 - 6	.24	.19 - 0.27	12	1800	1.4	8.9
		6 - 10	.27	.23 - 0.32	10	1400	1.4	8.9
		10 - 14	.27	.23 - 0.31	6	800	4.9	31
		14 - 19	.26	.23 - 0.30	4	600	6.5	41
100	9.8	0 - 1	0.25	0.14 - 0.29	12	1700	2.8×10^{-12}	18×10^{-15}
		1 - 2	.36	.22 - 0.38	7	1000	3.7	24
		2 - 3	.41	.23 - 0.44	5	720	5.2	33
		3 - 5	.35	.25 - 0.38	4	600	5.2	33
		5 - 8	.35	.26 - 0.37	3	400	6.4	40
200	4.9	0 - 1	0.40	0.30 - 0.49	4	600	11×10^{-12}	68×10^{-15}
		1 - 2	.60	.50 - 0.85	2	300	7.9	50
		2 - 3	.86	.80 - 0.93	1.5	210	12	76
350	2.0	0 - 1	1.00	0.45 - 1.16	1.1	160	22×10^{-12}	140×10^{-15}
		1 - 2	1.00	.65 - 1.05	.7	100	14	90
		2 - 3	1.03	.85 - 1.07	.4	60	16	100

TABLE 6. - COMPARISON OF FRICTION AND WEAR RATE DATA OBTAINED FROM DIFFERENT EXPERIMENTAL APPARATUS AND GEOMETRIES

Experimental apparatus	Composite wear specimen	Temperature, °C	Average friction coefficient	Specific wear rate, $m^3/N-m$
Self-aligning plain bearings	Molded[a] liner	25 315	0.15 .05	$1.2\pm0.4\times10^{-15}$ $1.2\pm0.4\times10^{-15}$
	Insert[a] liner	25 315	0.15 .05	$2.0\pm1.0\times10^{-15}$ $2.0\pm1.0\times10^{-15}$
Pin-on-disk	Pin[b]	25 350	0.24 .76	$0.38\pm0.27\times10^{-15}$ $41\pm25\times10^{-15}$
	Disk[c]	25 300	0.19 .05	$1.3\pm0.4\times10^{-15}$ $1.5\pm0.3\times10^{-15}$

[a]Data from Ref. 13.
[b]Data is geometric average of 25° and of 350° C data in Table 3.
[c]Data from Ref. 15.

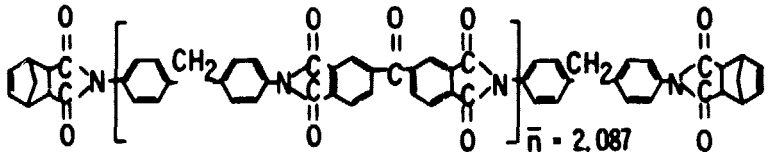

(a) IMIDIZED PREPOLYMER.

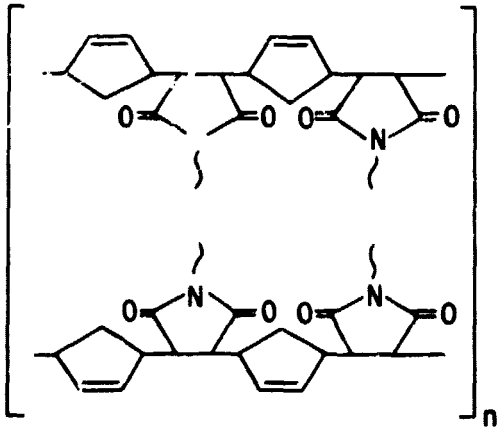

(b) CURED POLYIMIDE (IDEALIZED STRUCTURE).

Figure 1. - Addition-type of polyimide polymer (Type A) used in this study.

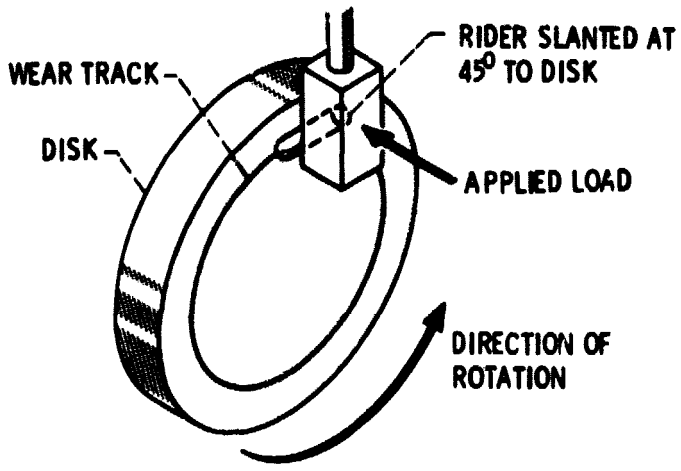

Figure 2. - Schematic diagram of friction specimens.

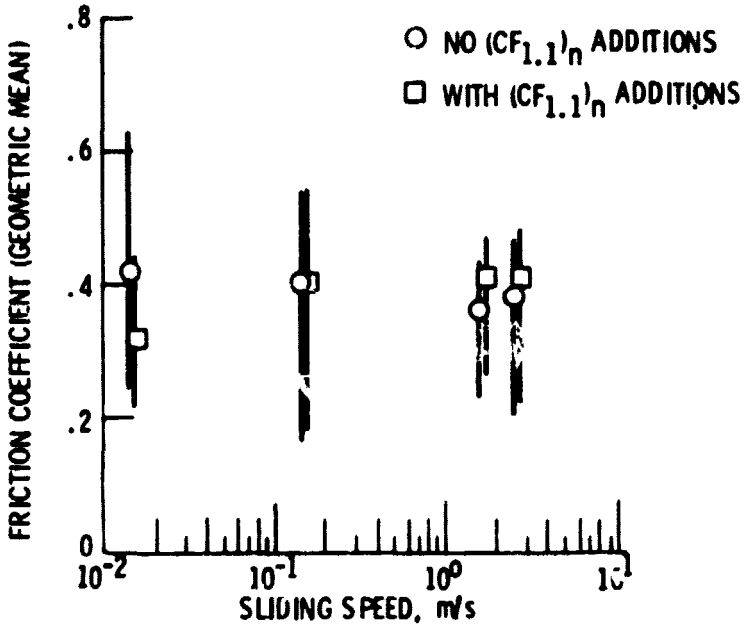

Figure 3. - Friction coefficient as a function of sliding speed for the Latin-square experimental data.

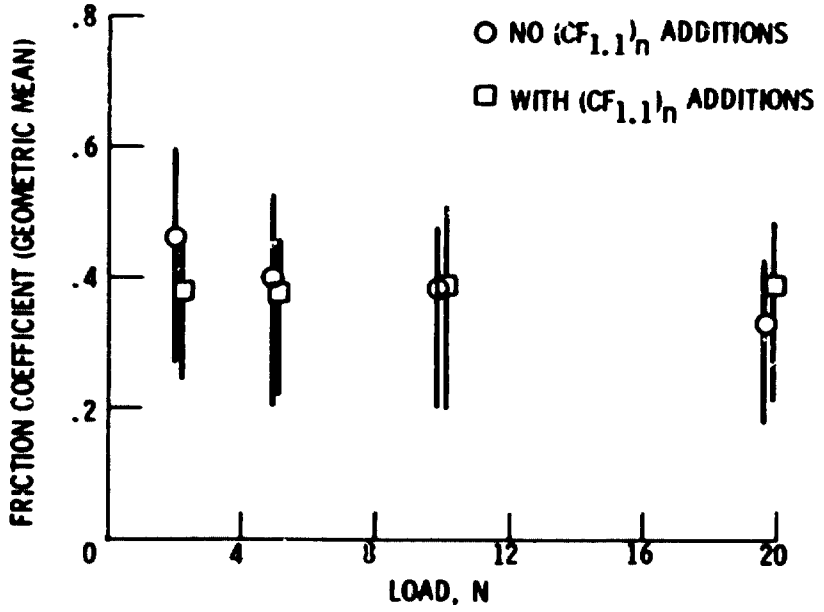

Figure 4. - Friction coefficient as a function of load for the Latin-square experimental data.

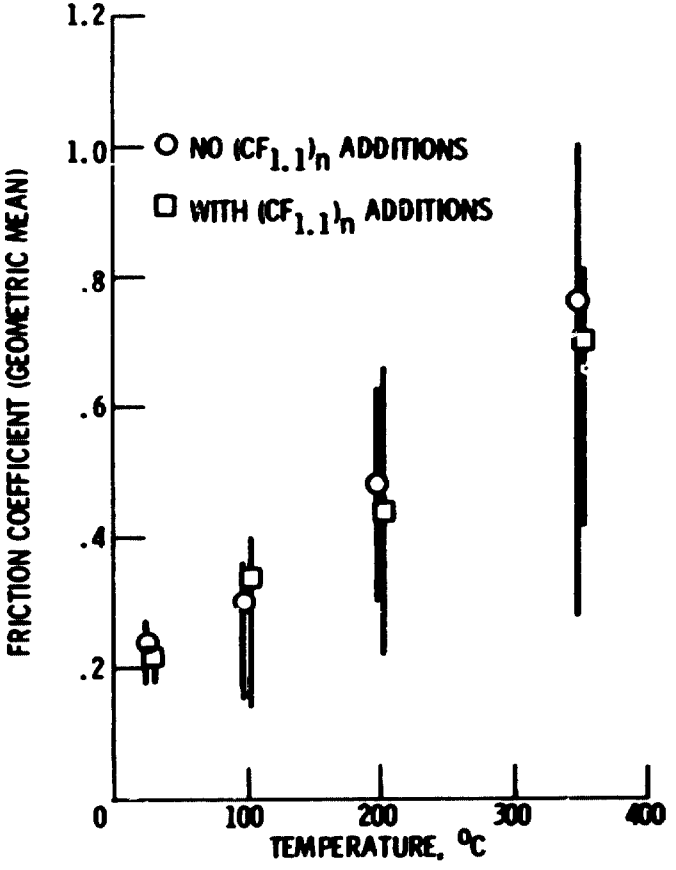

Figure 5. - Friction coefficient as a function of temperature for the Latin-square experimental data.

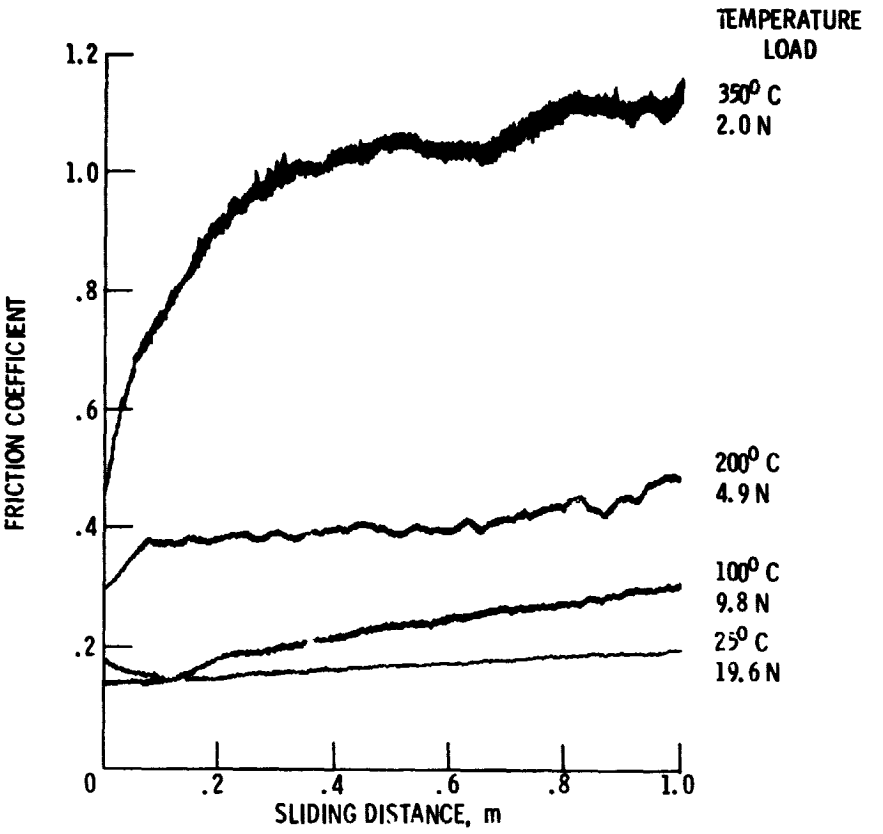

Figure 6. - Typical friction traces at a sliding speed of 1.7 m/s, showing the effect of sliding distance and temperature.

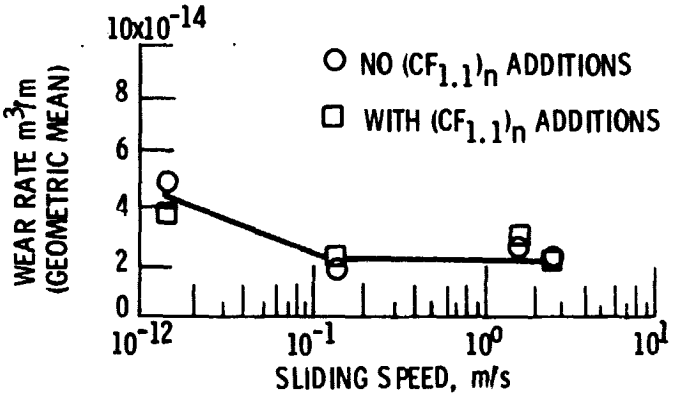

Figure 7. - GFRPI rider wear rate as a function of sliding speed for the Latin-square experimental data.

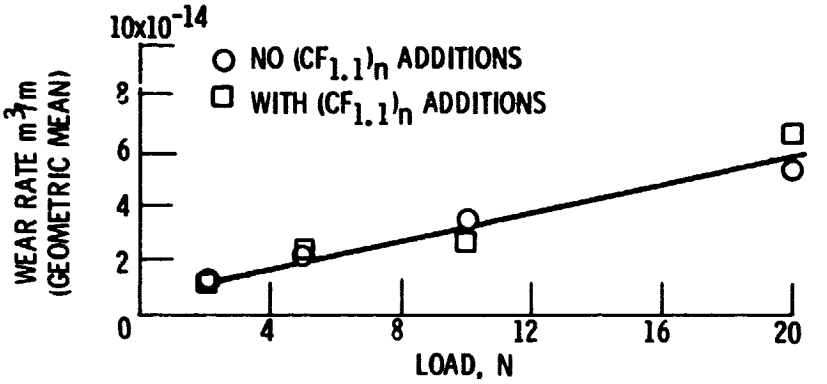

Figure 8. - GFRPI rider wear rate as a function of load for the Latin-square experimental data.

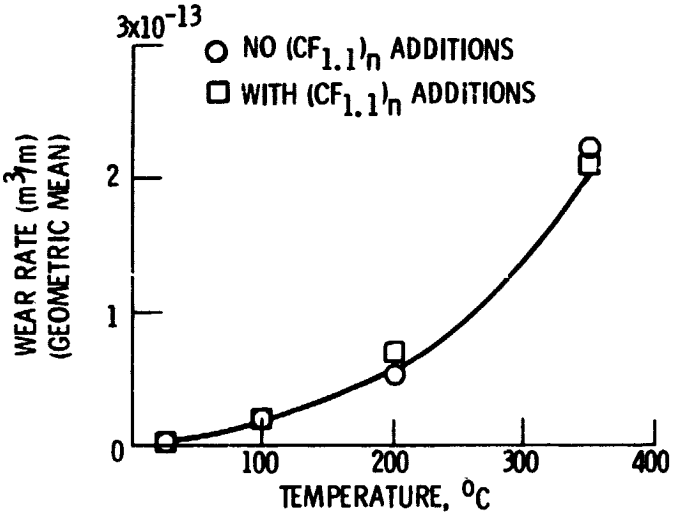

Figure 9. - GFRPI rider wear rate as a function of temperature for Latin-square experimental data.

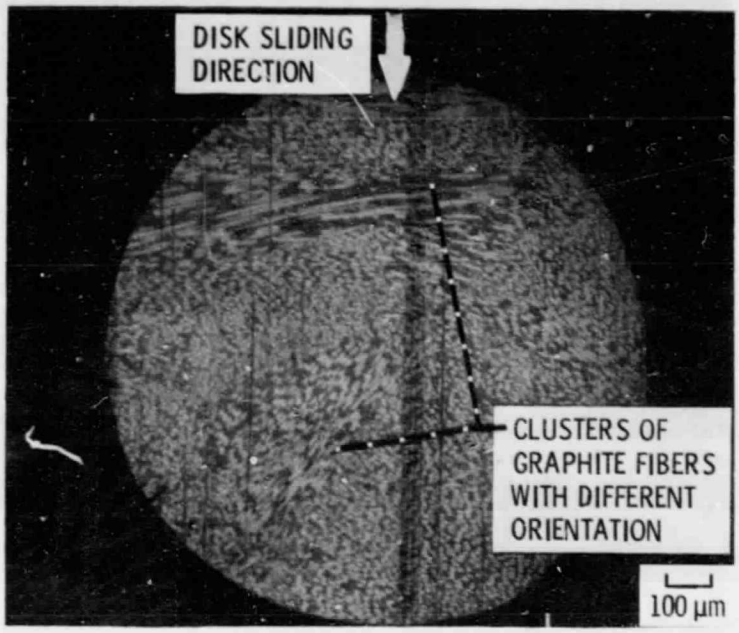

(a) OVERVIEW OF CONTACT AREA.

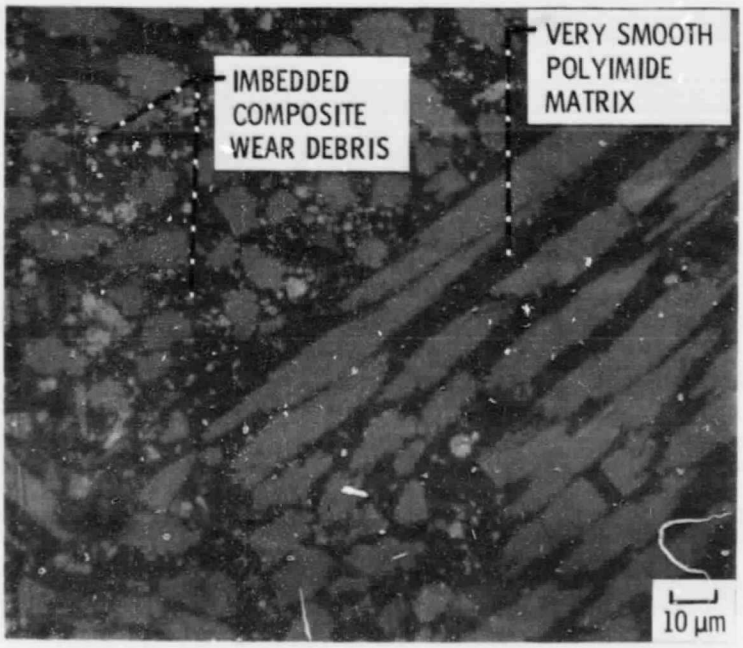

(b) HIGH MAGNIFICATION VIEW OF REGION WITHIN CONTACT AREA.

Figure 10. - Representative photomicrographs of the GFRPI rider contact areas for experiments conducted at 25° C. Experimental conditions: 4 km of sliding, 19.6 N load, and 1.7 m/s sliding speed.

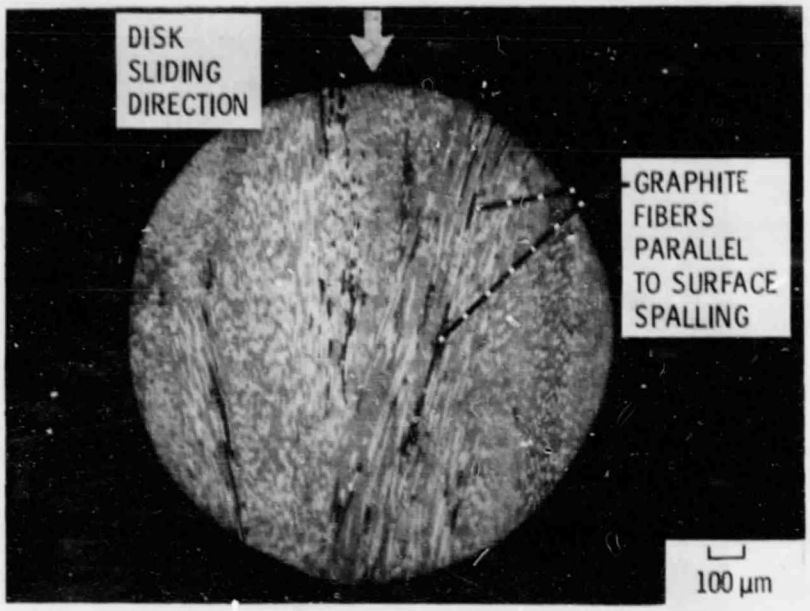

(a) OVERVIEW OF CONTACT AREA.

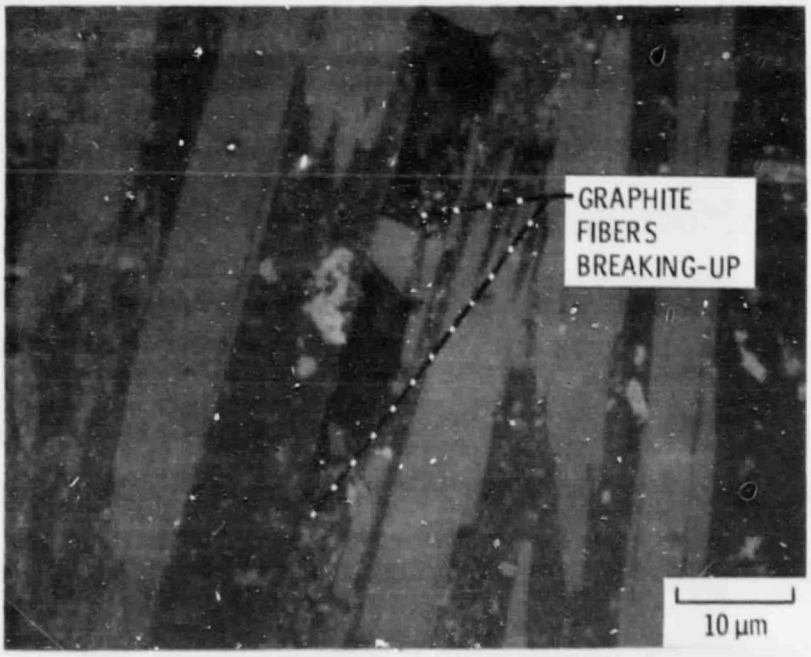

(b) HIGH MAGNIFICATION VIEW OF REGION WITHIN CONTACT AREA.

Figure 11. - Representative photomicrographs of the GFRP/ rider contact areas for experiments conducted at 100° C. Experimental conditions: 2 km of sliding, 9.8 N load, and 1.7 m/s sliding speed.

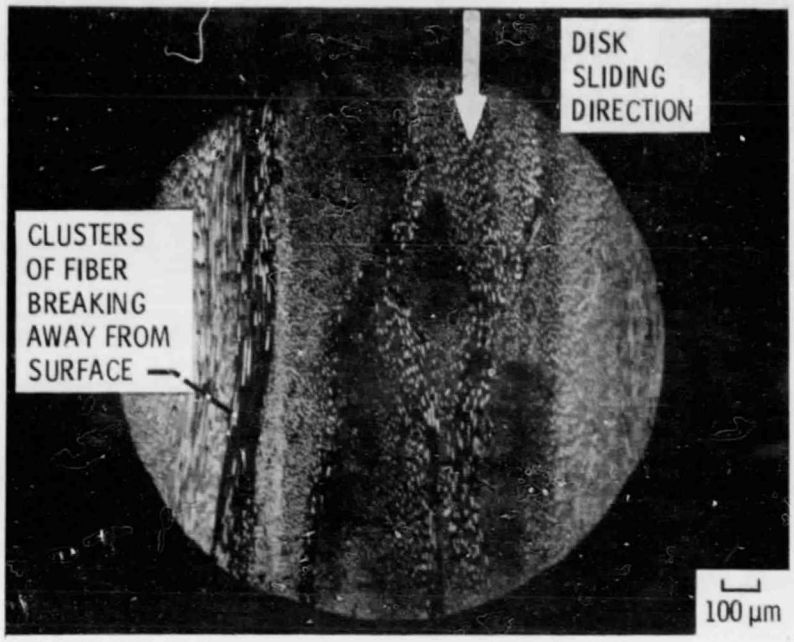

(a) OVERVIEW OF CONTACT AREA.

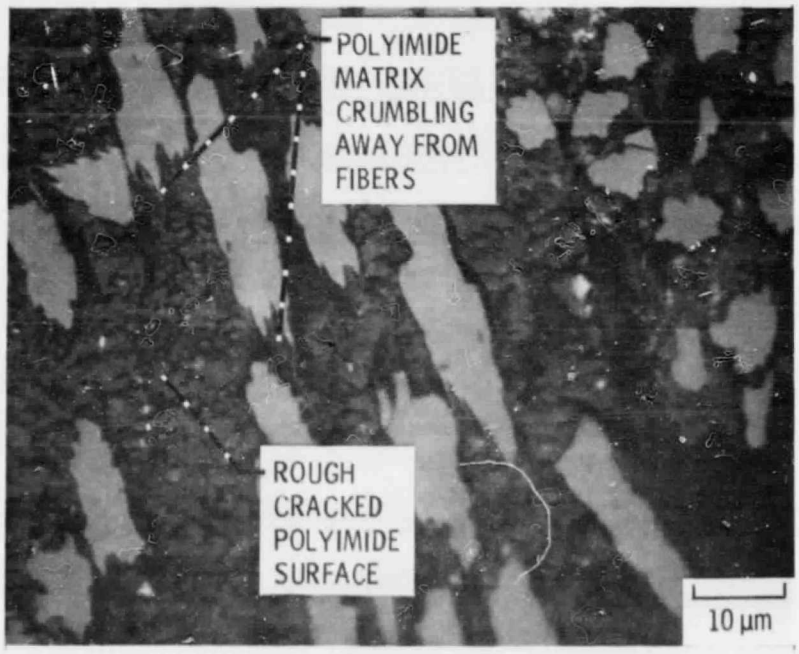

(b) HIGH MAGNIFICATION VIEW OF REGION WITHIN CONTACT AREA.

Figure 12. - Representative photomicrographs of the GFRPI rider contact areas for experiments conducted at 350° C. Experimental conditions: 1 km of sliding, 2.0 N load, and 1.7 m/s sliding speed.

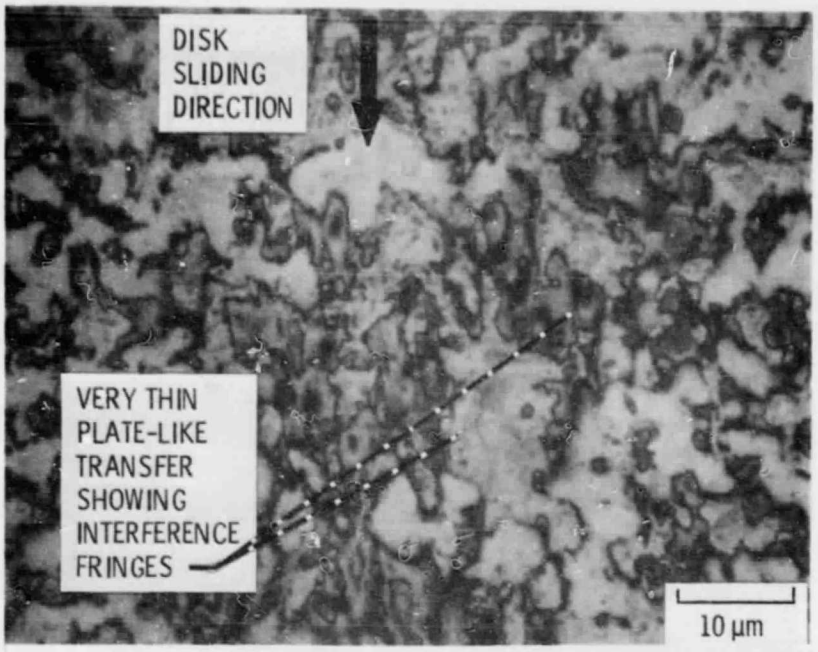

(a) 25^0 C.

(b) 350^0 C.

Figure 13. - Representative high magnification photomicrographs of the transfer from hemispherically tipped GFRPI riders to 440C HT stainless steel disks at 25^0 and at 350^0 C after 1 km of sliding.

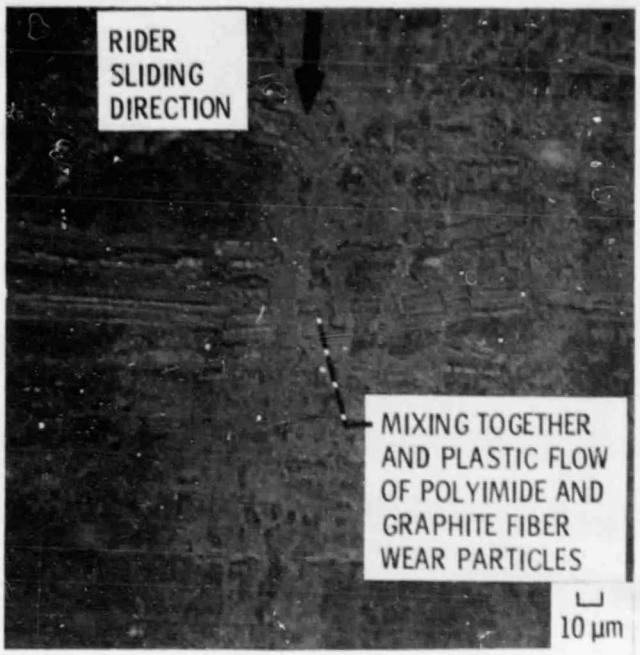

(a) 25° C.

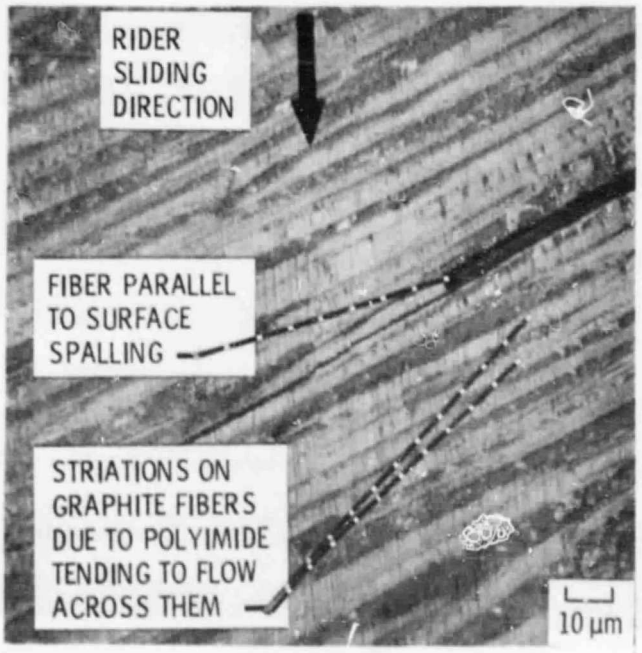

(b) 300° C.

Figure 14. - Representative high magnification photomicrographs of the wear surface on GFRPI disks at 25° and 300° C after 50 km of sliding.

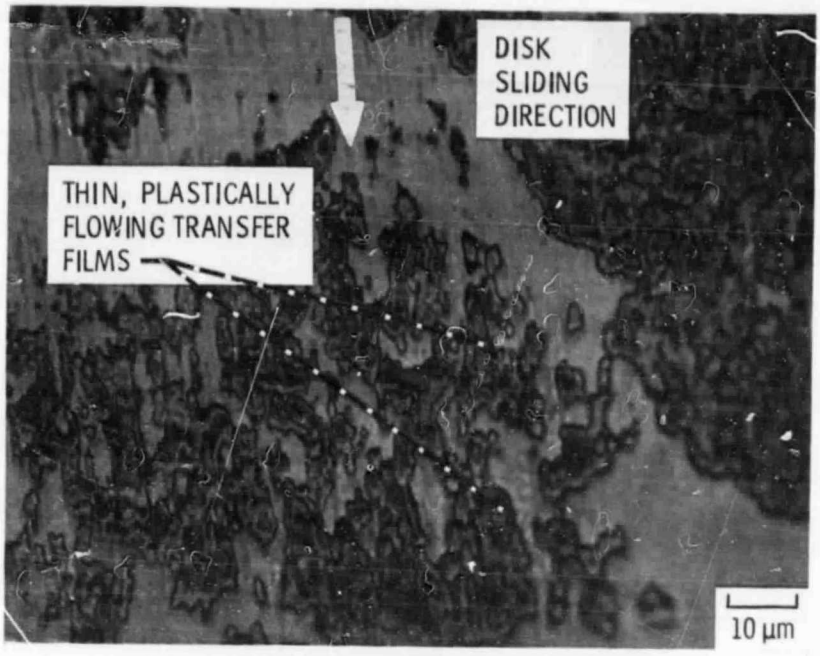

(a) 25° C.

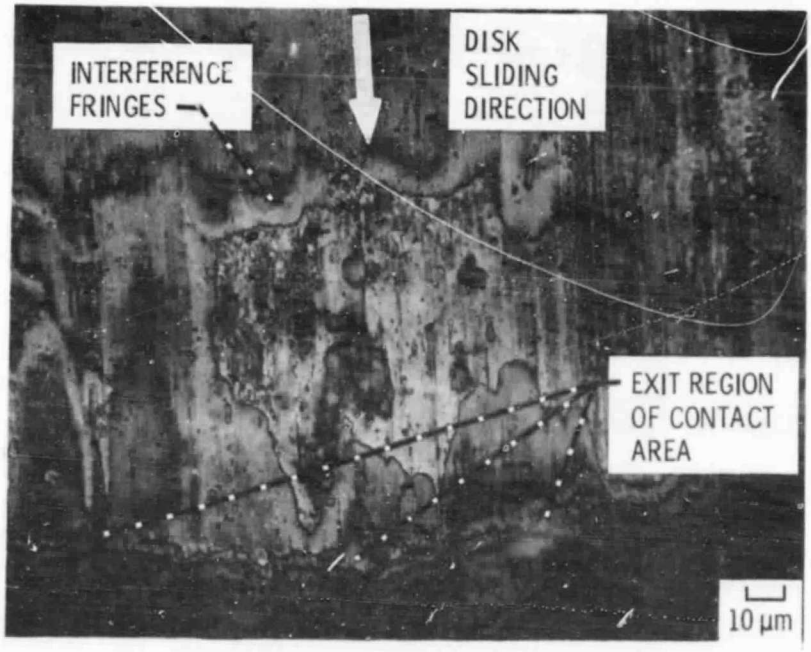

(b) 300° C.

Figure 15. - Representative high magnification photomicrographs of the transfer to 440C HT stainless steel hemispherically tipped riders sliding against GFRPI disks at 25° and 300° C after 50 km of sliding.